

AN ISOPERIBOLIC CALORIMETER TO STUDY ELECTROCHEMICAL INSERTION OF DEUTERIUM INTO PALLADIUM

KEYWORDS: *isoperibolic calorimetry, deuterium insertion, palladium electrode*

TURGUT M. GÜR,* MARTHA SCHREIBER,† GEORGE LUCIER,
JOSEPH A. FERRANTE, JASON CHAO,‡ and ROBERT A. HUGGINS§
*Stanford University, Department of Materials Science and Engineering
Stanford, California 94305-2205*

Received November 23, 1993

Accepted for Publication January 7, 1994

The design and the operational characteristics of a new isoperibolic calorimeter that is developed to study the electrochemical insertion of deuterium into palladium are described. The design is simple and involves inexpensive materials to build. It possesses a number of distinct advantages that makes it suitable for thermal measurements in other electrochemical systems. It is insensitive to the nature and the location of the heat source within the electrochemical cell. The calibration constant is found to be stable with $\pm 0.5\%$ uncertainty over a wide range of input power levels up to 22 W. It also has the capability of operating over a wide temperature range. In principle, the calorimeter can be used up to 600°C, provided that the electrochemical cell design and materials are chosen appropriately. The design also provides flexibility to adjust the sensitivity of the calorimeter according to the needs of the system under study.

I. INTRODUCTION

Calorimetry has been widely used in studying enthalpy changes during chemical and physical processes.¹⁻³ In general, the process under study takes

place inside the boundaries of the calorimeter proper at temperature T_c , which is in controlled thermal contact with its surroundings at temperature T_s through a heat transfer medium referred to as the K layer in this paper. The K layer can be chosen to have a desired value for thermal resistance depending on the type of calorimetry to be used. Electrochemical calorimetry⁴⁻⁷ has an added complication in that the cell inside the calorimeter proper usually requires electrical connections to an outside power source and/or measuring instruments.

After the initial announcement of Fleischmann and Pons,⁸ a number of groups⁹⁻¹³ including the Stanford University laboratory^{14,15} reported observation of excess power when deuterium was electrochemically inserted into palladium cathodes, while others¹⁶⁻¹⁹ reported the lack of experimental evidence. The early measurements in the Stanford University laboratory utilized "open" cells in a twin-type isoperibolic calorimeter where the behavior of light water and heavy water-based electrochemical cells have independently been studied and compared.^{14,15} While the palladium light water system showed no excess power, a significant amount of excess power was observed in the case of the heavy water system. More importantly, observations of significant amounts of excess energy of $\sim 10^7$ J/mol of palladium collected over extended periods of time were subsequently reported.²⁰⁻²⁴ These thermal measurements, recently reviewed by Storms,²⁵ were carried out by using a variety of calorimetric designs and techniques.

It is the purpose of this paper to describe and to discuss the design and the performance characteristics of a simple isoperibolic calorimeter developed in the Stanford University laboratory to study the thermal properties of the palladium-deuterium and palladium-hydrogen systems. This calorimeter may also be useful for other electrochemical and chemical systems in a wide range of temperatures up to 600°C.

*Current address: Center for Materials Research, Stanford University, Stanford, California 94305-4045.

†Current address: Daimler-Benz AG, 89013 Ulm, Germany.

‡Current address: Electric Power Research Institute, Palo Alto, California 94303.

§Current address: Zentrum für Sonnenenergie- und Wasserstoff- Forschung, Helmholtzstrasse 8, 7900 Ulm, Germany.

II. ELECTROCHEMICAL ISOPERIBOLIC CALORIMETRY

The word "isoperibol" denotes uniform surroundings. So, isoperibolic calorimetry refers to heat measurements in a calorimeter whose surroundings are maintained at a constant temperature. It utilizes a steady-state power balance method where heat is generated within the electrochemical cell placed inside the inner compartment and is conducted through a thermally conducting K layer into the outer compartment, which is maintained at a fixed lower temperature. Under steady-state conditions, a temperature distribution is established in which the temperature difference across the thermally conducting K layer between the two compartments transports heat at a rate that just balances the thermal power P_{therm} generated within the inner compartment. This can be expressed as

$$\text{thermal power generated} = P_{therm} = K(T_1 - T_2) , \quad (1)$$

where T_1 and T_2 are the temperatures of the inner and the outer compartments, respectively.

When power is introduced into the inner compartment electrically, the thermal power generated is equal to the applied electrical power P_{appl} , provided that the electrical power does not cause the occurrence of a chemical or electrochemical reaction that involves a change in the enthalpy of the system. This is the case when an open cell is used.

On the other hand, if a "closed" cell design employing an internal recombination catalyst is used, so that the enthalpy of the recombination reaction is contained in the inner compartment, P_{therm} and P_{appl} will be equal provided that there is no other heat generation process present. Any difference must be due to some additional power generation process taking place inside the electrochemical cell.

All the calorimetry results presented in this paper were obtained by using electrochemical cells of the closed type.

III. CALORIMETRIC PARAMETERS

The calibration constant, sensitivity, time constant, and linearity of a calorimeter are important parameters that govern its performance characteristics. In all calorimeters, heat is exchanged across the boundary between the calorimeter proper and its surroundings. Ideally, in isoperibolic calorimetry, this heat transfer is proportional to the temperature of the boundary such that

$$q = hA(T_c - T_s) , \quad (2)$$

where

q = rate of heat exchanged

h = heat transfer coefficient

A = area.

Equation (2) can be rewritten in the simple form

$$q = K\Delta T , \quad (3)$$

where K is the *calibration constant* for the calorimeter. This value needs to be determined accurately by carrying out careful measurements as described later in this paper.

Sensitivity S is a measure of the magnitude of the response ΔT of the calorimeter to a process under study and is defined by

$$S = \Delta T/q . \quad (4)$$

Note that this is the reciprocal of the calibration constant K . It is generally desirable to have a high sensitivity value, especially for measuring small changes in the heat flux. Sensitivity is usually given in units of degrees centigrade per watt or volts per watt.

The *time constant* τ of a calorimeter represents the time it takes for the initial temperature to relax to $1/e$ of its initial value upon stepwise decrease in the heat exchanged. This can be represented as

$$T_f = T_i \exp(-t/\tau) , \quad (5)$$

where T_i is the initial temperature and T_f is the final temperature.

Linearity refers to the range of temperature values where Eq. (3) still holds; i.e., the heat flux is linearly proportional to ΔT . It is desirable to operate the calorimeter in this range where K is constant.

IV. EXPERIMENTAL ASPECTS

IV.A. Isoperibolic Calorimeter Design

In an electrochemical cell under electrolysis conditions, the extent of the stirring in the electrolyte and the physical location at which heat is produced contribute to the extent of thermal inhomogeneity. This may lead to uncertainties in the thermal results since the temperature measurements may strongly depend on the location of the temperature probe.

A new type of isoperibolic calorimeter was designed to avoid these possible sources of error. It consists of two concentric heavy aluminum cylinders that are separated by a well-defined thermally conducting K layer. The inner cylinder contains an axial hole where the electrochemical cell under study snugly fits in. Under steady-state conditions, essentially all the heat generated within the electrochemical cell is forced to pass radially to the external environment through a pair of concentric heavy aluminum cylinders. Instead of relying on measurement of the temperatures within the electrochemical cell itself, this design involves the measurement of the temperatures of the two aluminum cylinders without having the need to assume a homogeneous temperature distribution within the cell. The large size and the excellent thermal conductivity of these aluminum cylinders assure uniformity of temperature within the

cylinders regardless of the location of the heat source within the electrochemical cell. So, possible sources of error related to such issues as the amount of stirring and the exact locations of the heat sources and the temperature probes within the electrochemical cell are avoided.

The schematic design of the isoperibolic calorimeter including the electrochemical cell is shown in Fig. 1. The inner (T1) aluminum cylinder has an outer diameter of 2 in., an inner diameter of 1.16 in., is 4 in. long, and weighs ~365 g. The outer (T2) aluminum cylinder is 7 in. long, weighs 958 g, has an inner diameter of 2.25 in., and has an outer diameter of 3.0 in. Thus, the gap across which the controlled heat conduction takes place and across which the temperature difference is measured is only 0.125 in. The electrochemical cell that fits snugly inside the T1 cylinder is made of a quartz tube 1.14 in. (29 mm) in outside diameter and 4 in. long. A sheet of aluminum foil wrapped around the quartz cell ensures good thermal contact with the T1 aluminum cylinder.

The T1 cylinder housing the electrochemical cell is mounted on Teflon supports and placed concentrically

inside the T2 cylinder in such a way that 1.5 in. of vertical space is left above and below the T1 cylinder. This vertical space above and below as well as the 0.125-in.-wide radial gap between the two cylinders is packed with dry Al_2O_3 powder (J. T. Baker) while the outer surface of the T2 cylinder is gently tapped to assure uniform packing. This 1.5-in.-thick Al_2O_3 insulation above and below the T1 cylinder provides thermal insulation and thus forces the heat to be transferred in the radial direction through the K layer to the outer cylinder. The effective thermal conductivity of this Al_2O_3 powder, which has a particle-size range of 50 to 200 μm , is experimentally determined to be $\sim 1.6 \times 10^{-3} \text{ W/cm} \cdot ^\circ\text{C}$. The thermal conductivity of the Al_2O_3 powder is very much dependent on its moisture content. Hence, care must be taken to avoid moisture getting into the calorimeter during prolonged experiments. A sturdy and pinhole-free plastic bag wrapped tightly around the calorimeter in the water bath is found to be useful for this purpose. Periodic calibration of the calorimeter alleviates the concern about uncertainty in the stability of the calibration constant.

Three small thermocouple holes $\frac{1}{16}$ in. in diameter are drilled vertically down to half-height of each aluminum cylinder. The holes are located at midpoints of the wall thickness of the cylinders and are spaced 120 deg circumferentially from each other. A few drops of silicone oil is put at the bottom of these holes to provide good thermal contact between the thermocouples and the aluminum cylinders. Copper-constantan (Type T) thermocouples are firmly fixed into these holes to make good physical contact with the aluminum at the bottom of the holes. The thermocouples are connected in a differential mode such that only the copper legs of the thermocouples are wired to the copper inputs of the digital microvoltmeters. Thus, all possible adverse thermoelectric contributions from dissimilar joints in the temperature measuring circuitry are eliminated. Each calorimeter is equipped with four pairs of thermocouples. Two pairs are connected between the T1 and the T2 aluminum cylinders so that only the temperature difference between the cylinders is measured by two independent thermocouple pairs. The other two pairs of thermocouples are connected between each aluminum cylinder and the surrounding constant temperature water bath to measure the differential temperatures of each cylinder with respect to the water bath. A $6\frac{1}{2}$ digit Keithley Model 193A microvoltmeter is used for reading the thermocouple output, and its precision is found to be 0.1°C .

Eight such calorimeters have been built. The $1/e$ time constants of the calorimeters were determined from the transient behavior of the temperature in response to step changes in the level of the input power and were found to range between 13 and 15 min. This is a reasonably rapid response time. Since the outer aluminum cylinder is kept at a constant temperature throughout the calorimetric measurements, it does not

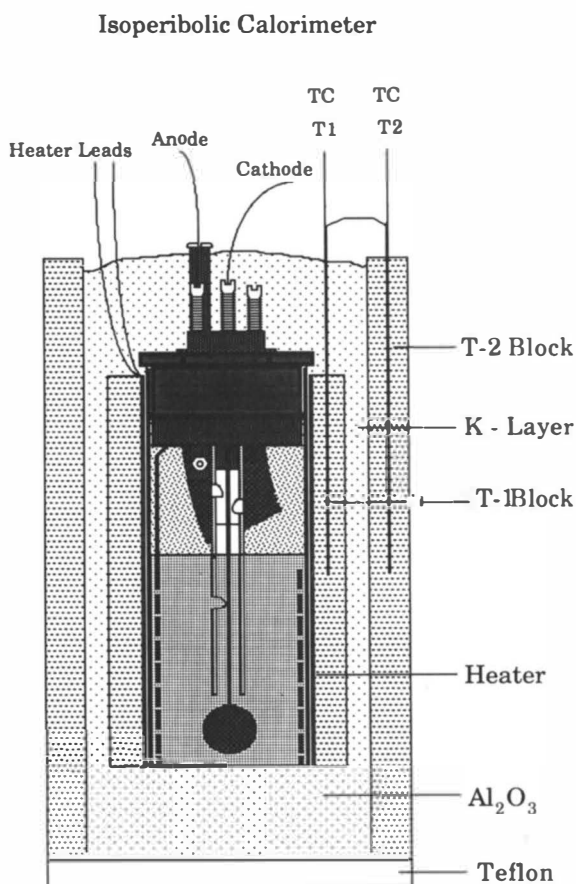


Fig. 1. Schematic design of the isoperibolic calorimeter featuring an external thin sheet joule heater wrapped around the electrochemical cell and inserted inside the inner aluminum cylinder.

participate in the transient behavior and hence does not contribute to the response time.

IV.B. Electrochemical Cell Design

The electrochemical cells used in this work are closed cells; i.e., they contain an internal catalytic recombination device made of platinum/nickel supported on a Teflon sheet to recombine the D_2 and the O_2 that have been electrolyzed and to return it by gravity back into the electrolyte. This recombination catalyst is of the general type that is used in maintenance-free car batteries. By contrast, the gaseous products of electrolysis are vented off to the outside in open cells. The internal recombination catalyst had a geometric area of $\sim 10 \text{ cm}^2$ and was suspended from the cell cap in the vapor phase above the electrolyte.

The cell container was a cylindrical quartz tube 2.9 cm (1.14 in.) in outside diameter and 10 cm (4 in.) tall. All the cells were connected externally to silicone oil bubblers by a plastic tubing. This served two purposes. The bubbler system allowed the escape of gas in the amount of uncombined oxygen during the initial moments of electrolysis. The other aspect was to prevent atmospheric moisture to diffuse back into the electrolyte in the electrochemical cell containing about 20 ml of 0.1 M LiOD in D_2O . This is an important consideration since hydrogen exchanges readily with deuterium and is selectively absorbed into the palladium cathode.

Three different types of cell designs were used to demonstrate that the way the power is generated inside the electrochemical cell has no bearing on the calibration constant. In the first design, a static immersion joule heater shielded in a J-shaped quartz tubing was used for providing the joule heating for calibration. The cell was sealed with a rubber stopper that housed the feedthrus for cathode and anode lead connections, the immersion joule heater, and the gas vent to the silicone bubbler external to the cell. The anode was a 0.010-in.-thick, ~ 200 -cm-long platinum wire spirally wound inside the cell. The anode-to-cathode surface area ratios were between 10 and 15 to assure that most of the applied voltage drop was on the palladium cathode.

Although this general design provided reproducible calibration, the problems associated with the management of the space inside the cell as well as on the rubber stopper and the occasional and unpredictable breakage of the quartz shielding around the joule heater lead to a modified design.

The second design used a modified three-electrode design in which electrolysis heating was utilized for calibration purposes. Again, rubber stoppers were used to support the electrical feedthrus and the gas vent to the bubbler. The cell design used a spirally wound palladium ribbon anode, the usual palladium cathode, and an additional platinum cathode to provide the heat for calibration by electrolysis. The palladium anode was

common to both the palladium and the platinum cathodes. There was no electrical cross talk between the two electrodes. This is illustrated in Fig. 2, which shows the influence of the heater power on the cell electrolysis power. At the several levels of cell power indicated in Fig. 2, the heater power was varied at three levels over a wide range between 4 and 10 W. The data clearly indicate that the cell electrolysis power levels were unaffected by the changes in the heater power levels.

The third design used a simple palladium cathode/palladium ribbon anode arrangement inside the cell. The joule heater power for calibration was provided by a thin sheet heater wrapped externally around the quartz container covering most of its area and snugly fitted between the cell and the inner aluminum cylinder of the calorimeter. Rubber stoppers were replaced by cell caps machined out of Delrin^R equipped with suitable feedthrus.

The palladium (Engelhard) cathodes were prepared by repeated arc melting in an argon atmosphere, followed by mechanical deformation to produce a "fat dime" shape. During the initial stages of the experiments, thin platinum and gold wires were employed for electrical connection to the palladium cathode. However, energy dispersive spectroscopy studies on the surface of the palladium cathodes indicated the presence of substantial amounts of platinum and gold coverage, which blocks deuterium insertion into the palladium electrode. Consequently, fine palladium wire ~ 0.005 in. in diameter and shielded by a thin Teflon tube was used as the cathode current collector. Similarly, the fine wire platinum anodes were replaced by large surface area thin palladium ribbon anodes, produced by rolling a $\frac{1}{8}$ -in.-o.d. palladium wire.

IV.C. Calorimeter Calibration Principle

In a closed cell with no electrolysis taking place, calibration with a joule heater gives

$$K = P_{hr} / \Delta T_{hr} \quad (6)$$

The procedure involves the introduction of several levels of joule heating power and the steady-state measurement of corresponding rises in the temperature. Then, a plot of P_{hr} compared with ΔT_{hr} gives a linear relation the slope of which is equal to the calibration constant. The situation, however, is more involved if electrolysis is also taking place during calibration. This is because the cell resistance changes with temperature as the total power level input to the cell changes. This change occurs regardless of whether the electrolysis process is carried out under potentiostatic or galvanostatic conditions.

Under electrolysis conditions, the total power P_{tot} put into the cell during calibration is due to the heater P_{hr} and the electrolysis power P_{el} :

$$P_{tot} = P_{hr} + P_{el} \quad (7)$$

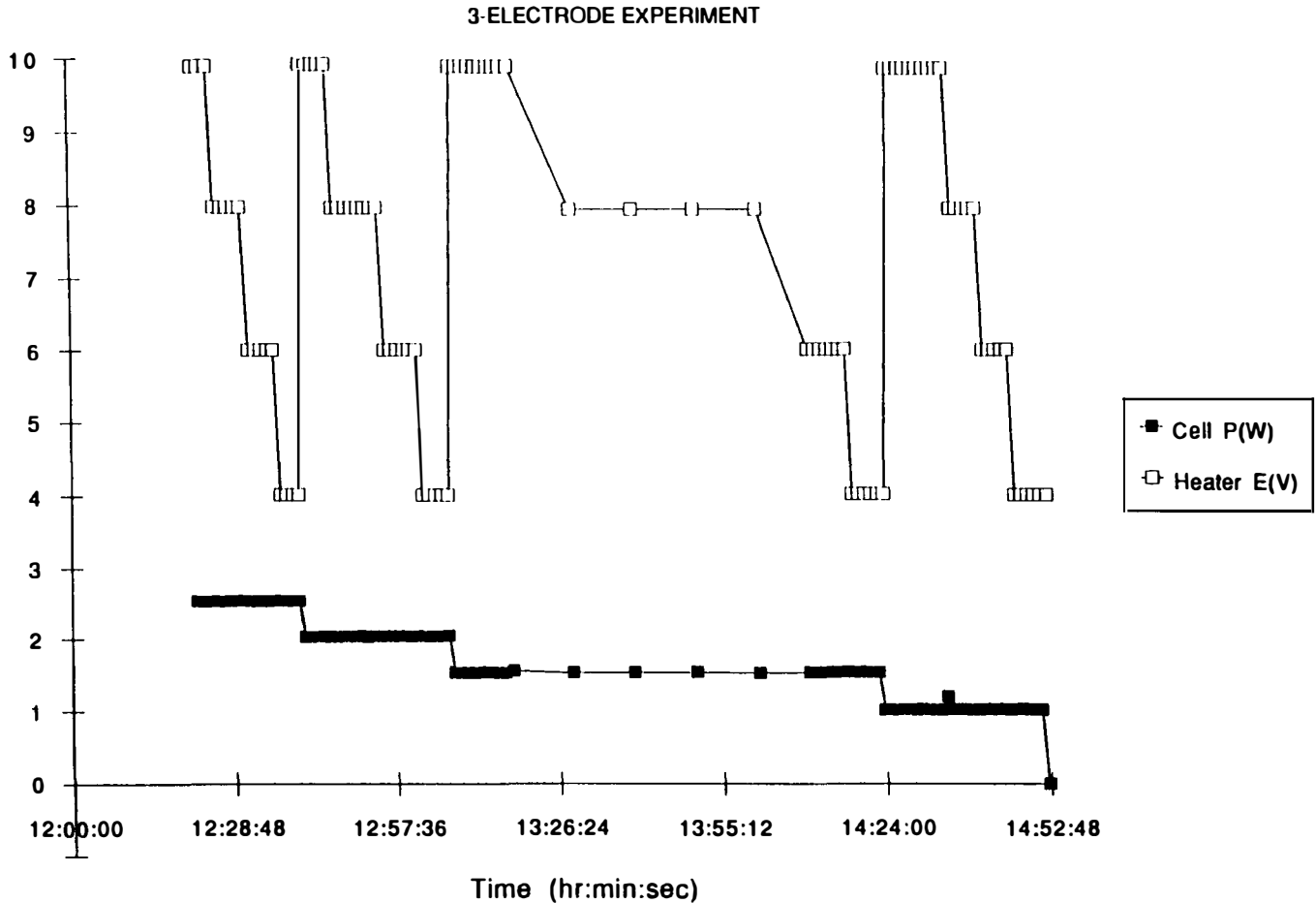


Fig. 2. Verification of the cross-talk issue between the electrolytic heater and the electrolysis power levels. Data clearly indicate that the heater and the cell power levels can be varied independently of each other without interference.

This additional joule heater power increases the cell temperature by ΔT_{htr} such that the total temperature rise ΔT_{tot} is given by

$$\Delta T_{tot} = \Delta T_{htr} + \Delta T_{el} . \quad (8)$$

As a result of the increased temperature, the electrolyte resistance decreases, and the electrolysis current will increase if the electrolysis voltage is maintained constant. This increases the electrolysis power input by δP_{el} such that

$$P_{el} = P_{el)0} + \delta P_{el} , \quad (9)$$

where $P_{el)0}$ denotes the initial electrolysis power level prior to the introduction of joule heating power for calibration. One can determine this new value P_{el} precisely by measuring the electrolysis voltage and current. The corresponding temperature rise corrected for this change in the electrolysis power level is given by

$$\Delta T_{el} = \Delta T_{el)0} + \delta T_{el} . \quad (10)$$

It is not so easy to independently measure ΔT_{el} . However, one can determine this value as shown below.

Note that for the case of electrolysis under constant voltage, i.e., potentiostatic conditions, the corrections δP_{el} and δT_{el} are both positive in sign giving rise to increased values of electrolysis power and temperature.

On the other hand, if the electrolysis is conducted under constant current, i.e., galvanostatic conditions, the cell voltage and hence the electrolysis power will decrease because of the decrease in the cell resistance. Hence, corrections δP_{el} and δT_{el} are both negative in sign under these circumstances.

Earlier work at the Stanford University laboratory that also involved isoperibolic calorimetry on open electrochemical cells demonstrated that the temperature rise depended linearly on the power^{13,14} such that

$$\Delta T_{el} = P_{el} \Delta T_{el)0} / P_{el)0} . \quad (11)$$

Hence, the calibration constant corrected for either the potentiostatic or the galvanostatic electrolysis conditions is given by

$$K = P_{htr} / (\Delta T_{tot} - P_{el} \Delta T_{el)0} / P_{el)0} . \quad (12)$$

An alternative strategy is to operate the cell under constant electrolysis power mode. The electrolysis power can be maintained constant during calibration by joule heating by the use of a computer-controlled feedback program. Then, the observed temperature rise would be due to the effect of the joule heater alone since the electrolysis power is unchanged when the heater power is introduced. Under these circumstances, the corrections δP_{el} and δT_{el} are both zero, and the calibration constant is simply given by

$$K = P_{hr} / (\Delta T_{tot} - \Delta T_{el}) . \quad (13)$$

Note, however, that the relation between the electrolysis voltage and the current will change even under constant electrolysis power mode because the cell resistance changes when joule heater power is introduced during calibration.

IV.D. Calibration Procedure

The calorimeters were calibrated by using three different methods of introducing power, namely, immersion joule heater, electrolysis, and external joule heater. The purpose was to demonstrate that the way the power is generated inside the electrochemical cell has no bearing on the calibration constant. The calibration procedure simply involved the introduction of several levels of joule heating power, both in increasing and decreasing steps, and the measurement of the corresponding temperature difference between the two aluminum cylinders in each case. For most cases, calibrations were carried out while electrolysis was also taking place, except when starting a fresh new electrochemical cell.

Calibrations were carried out usually under constant electrolysis power mode, although constant voltage operation was also employed at times. However, corrections to the temperature and electrolysis were always made to accurately determine the calibration constant.

IV.E. Measurement and Data Acquisition System

Figure 3 schematically depicts the measurement and the data acquisition system. The power for both the electrolysis and the joule heater were supplied by Lambda LLS series power supplies. These power supplies were configured such that they were computer controlled to maintain constant electrolysis power regardless of the level of joule heater power put in for calibration. A Mac IIx computer was used for this purpose as well as to acquire data from the calorimeters monitored by a Keithley 193A DMM microvoltmeter connected to a Keithley 706 Scanner. For each calorimeter, a total of ten experimental parameters consisting of four differential and two absolute thermocouple values as well as two voltage and two current (read as voltage across precision resistors) values were measured continuously, averaged over ten readings and stored ev-

ery 5 to 15 s. The voltage values were measured immediately above the cell caps. Similarly, the current values were monitored as voltage drops across high wattage 1- Ω precision resistors located right above the cell caps. The hardware allowed five calorimeters to be monitored and controlled simultaneously. All five calorimeters sit inside a constant temperature water bath. Both the cell operation and the data acquisition were controlled by using the LabView software from National Instruments Company.

V. RESULTS

Two sets of typical calibration data, covering a period of nearly 3 days, taken during a calibration run involving a fresh, unused, and unloaded palladium cathode is shown in Fig. 4. The variation of the cell electrolysis and the calibration heater power levels as well as the values of the three differential temperatures are plotted as a function of time. The calibration procedure was initially started with no electrolysis taking place on the fresh palladium cathode. Three increasing and two decreasing steps of external joule heater power were applied as shown in Fig. 4a. The corresponding temperature values T-1, T-2, and DTB show flat and stable behavior as expected. Then, the electrolysis power was turned on under constant power mode. The joule heater calibration power was added on top of the electrolysis power in three increasing and three decreasing steps as shown in Fig. 4b. The transient before stabilization at the new power level was ignored, and all the power and temperature data clearly showed flat and time-independent behavior as expected. This illustrates the steady and reliable performance of the calorimeter over extended periods of time.

V.A. Temperature Distribution

The temperature distribution within the calorimeter is measured by the use of four copper-constantan (Type T) thermocouples located at different positions in the calorimeter as described in Sec. IV.A. The thermocouples are configured in a differential mode such that only the copper ends of each pair are connected to the microvoltmeter thus eliminating spurious thermoelectric effects. Figure 5 shows the exceptional agreement between three temperatures measured between six points in the calorimeter by four pairs of differential thermocouples. The data illustrate the typical time-dependent variation of the temperature during a calibration carried out by the use of an immersion-type joule heater. Note also that the temperatures T-1 and T-2 were both measured in a differential mode with respect to the water bath. Thus, (T1 - T2) is the differential temperature between the two aluminum cylinders. Similarly, DTA and DTB denote the other two sets of differential temperatures. The temperature measurements

were taken at three locations 120 deg apart along the circumference of the aluminum cylinders.

Figure 5 clearly demonstrates the uniformity of the temperature distribution within the calorimeter and in particular within the inner aluminum cylinder. This is an important advantage. It eliminates the ambiguity about the exact locations of the source of heat and the temperature probe within the calorimeter. Hence, the extent of stirring within the electrochemical cell becomes irrelevant and immaterial.

V.B. Calibration Constant

To illustrate the relationship between the calibration power and the calibration constant, the variation of power during a calibration experiment is shown in Fig. 6a, which is the same set of data presented in Fig. 4b chosen for the purpose of being consistent. It is slightly modified to make it easy to visually correlate the variation of the calibration constant with the input power level. This modification consists of stripping the

Computerized Data Acquisition System

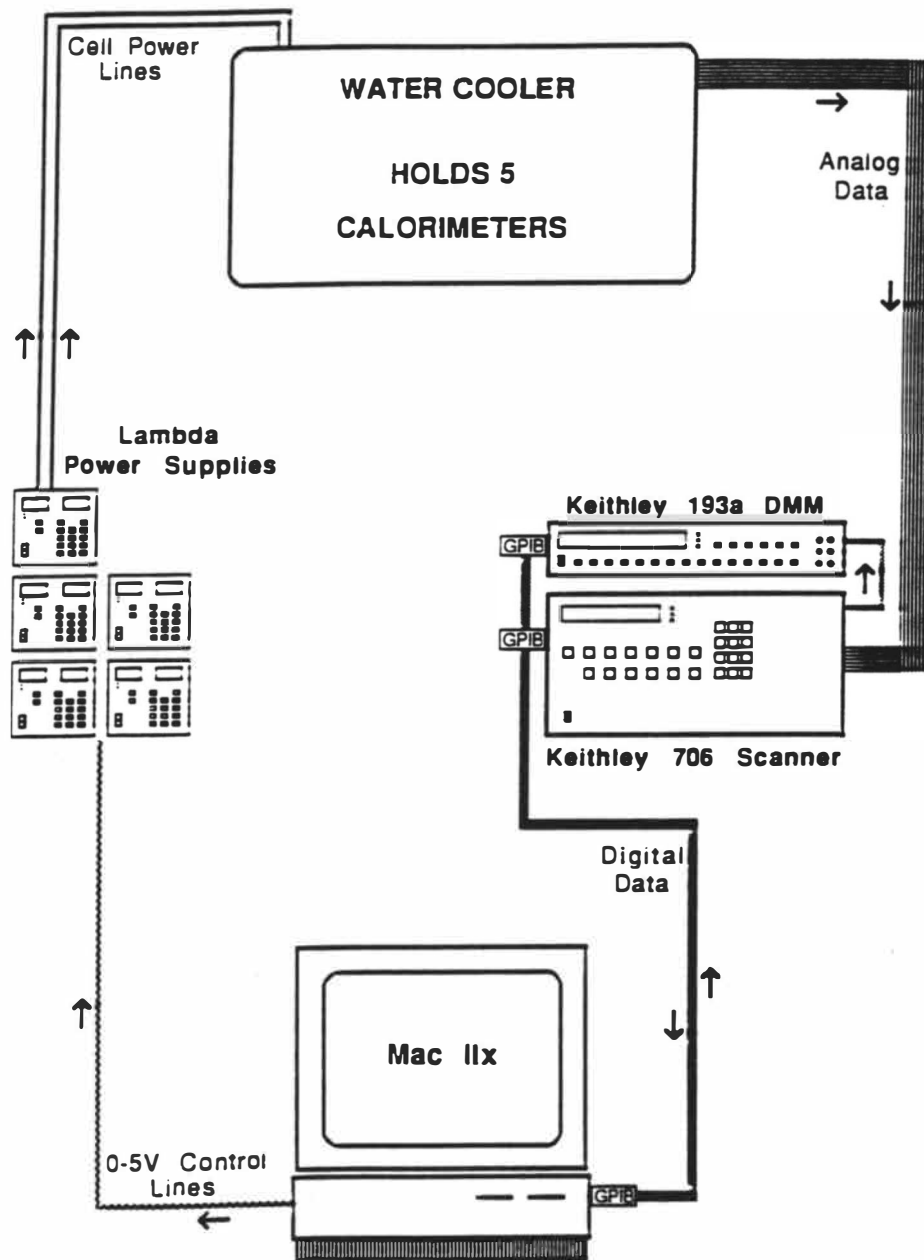
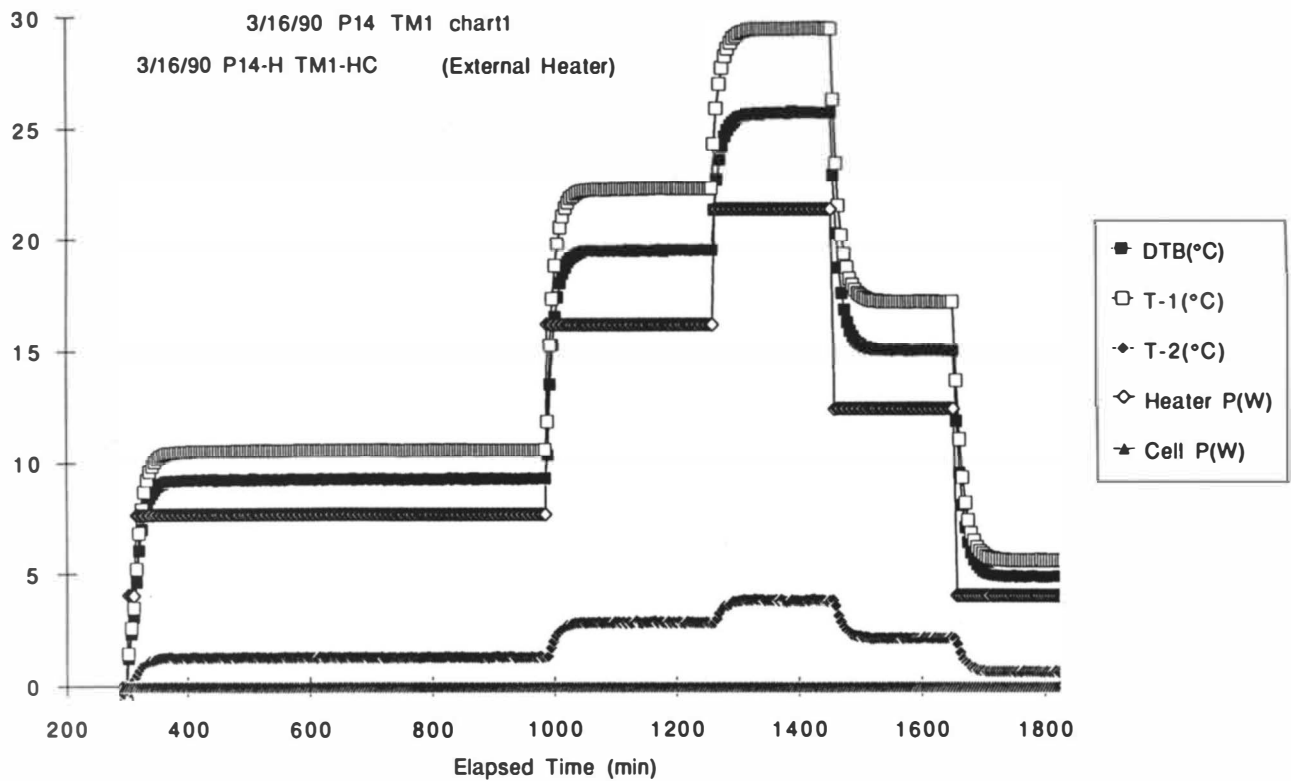
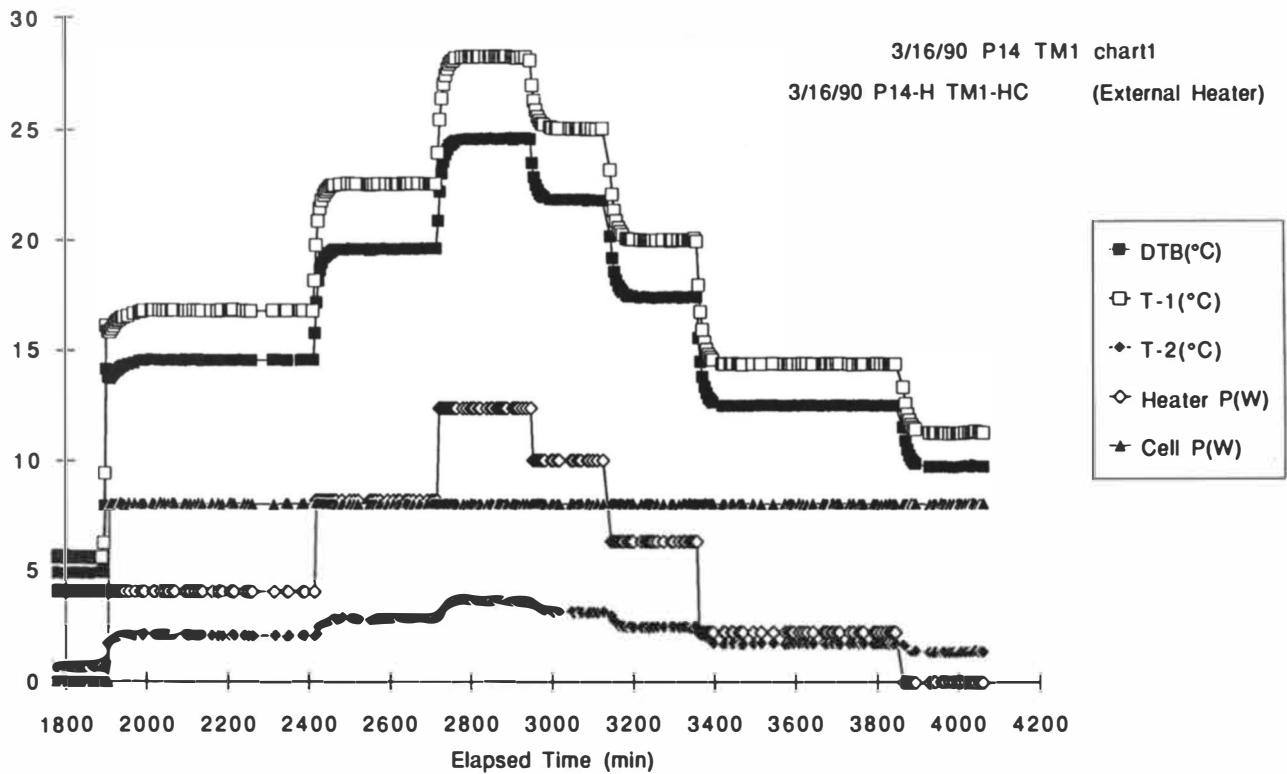


Fig. 3. The schematic diagram of the electrical measurements and the data acquisition system for the calorimetry experiments.



(a)



(b)

Fig. 4. Time-dependent behavior of the three temperatures and the two power levels for a typical calorimetric experiment (a) initially with no electrolysis and (b) with electrolysis taking place. DTB denotes the differential temperature measured across the two aluminum cylinders. T1 and T2 are the differential temperatures of the inner and outer aluminum cylinders, respectively, measured with respect to the bath. The vertical axis indicates the magnitudes of the power and the temperature parameters in watts and degrees centigrade, respectively.

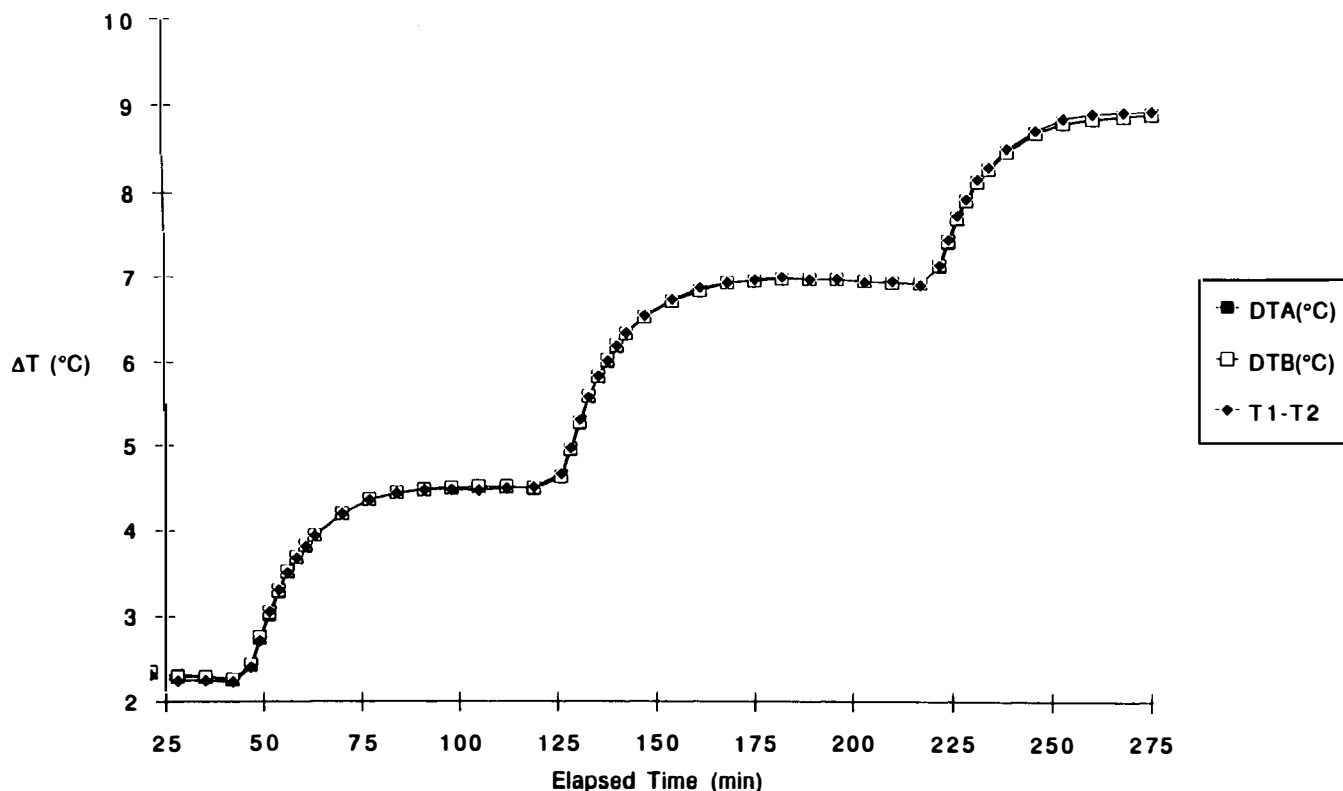


Fig. 5. The variation of temperature with time during a calibration experiment at three levels of power input by using an immersion joule heater. All three differential temperatures, measured at different locations that are circumferentially 120 deg apart, lie exactly on top of each other, which indicates a uniform temperature distribution within the inner aluminum cylinder in the calorimeter.

actual experimental data symbols off the curves for various input powers and simply connecting the data points by lines. The joule heat for calibration is supplied to the calorimeter by the external thin sheet heater. The electrolysis for this experiment was carried out under constant electrolysis power mode. Figure 6a shows the electrolysis power, the heater power, and their sum as a function of time. Note that all are very flat and steady with time. High total power levels sometimes in excess of 20 W, as is the case here, are commonly used in both the calibration as well as the electrochemical insertion experiments.

The time dependence of the calibration constant extracted from these data by using Eq. (31) is shown in Fig. 6b. The spikes on the graph represent the transient behavior of the calorimeter when the input power level is varied abruptly. The steady-state behavior, however, clearly shows that the calibration constant values are very consistent, lying in a band $\sim 1\%$ wide, and independent of the input power level as well as of time.

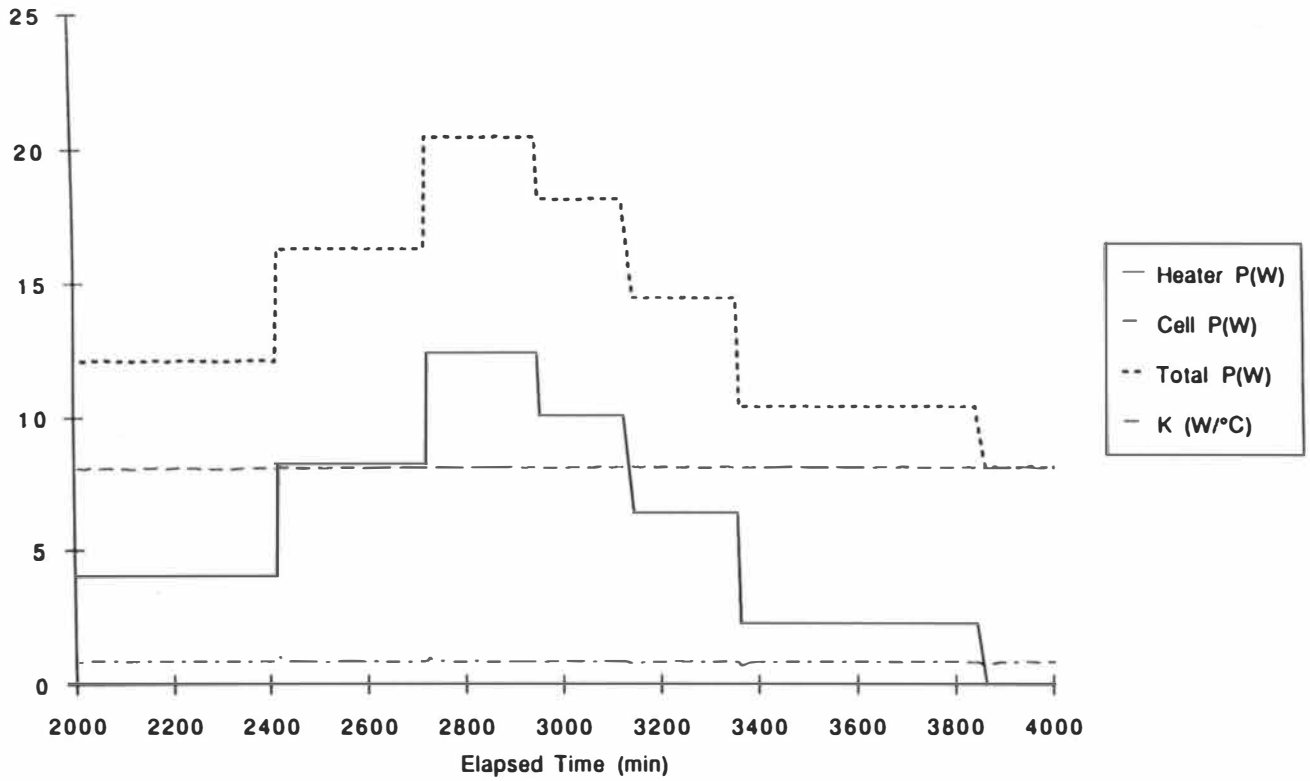
The effect of different types of joule heating on the calibration constant was also studied. It was found that the value of the calibration constant was independent of the manner in which calibration joule heat was supplied to the calorimeter. This is illustrated in Fig. 7,

which compares the results of calibration experiments by using the external thin sheet joule heater with that of the electrolytic heater, with and without simultaneous electrolysis taking place. Over a very wide range of power levels, the calibration constant is independent of the type of calibration heat source, and in this particular calorimeter is equal to $0.830 \text{ W}/^\circ\text{C}$ with a standard deviation of $\pm 0.5\%$.

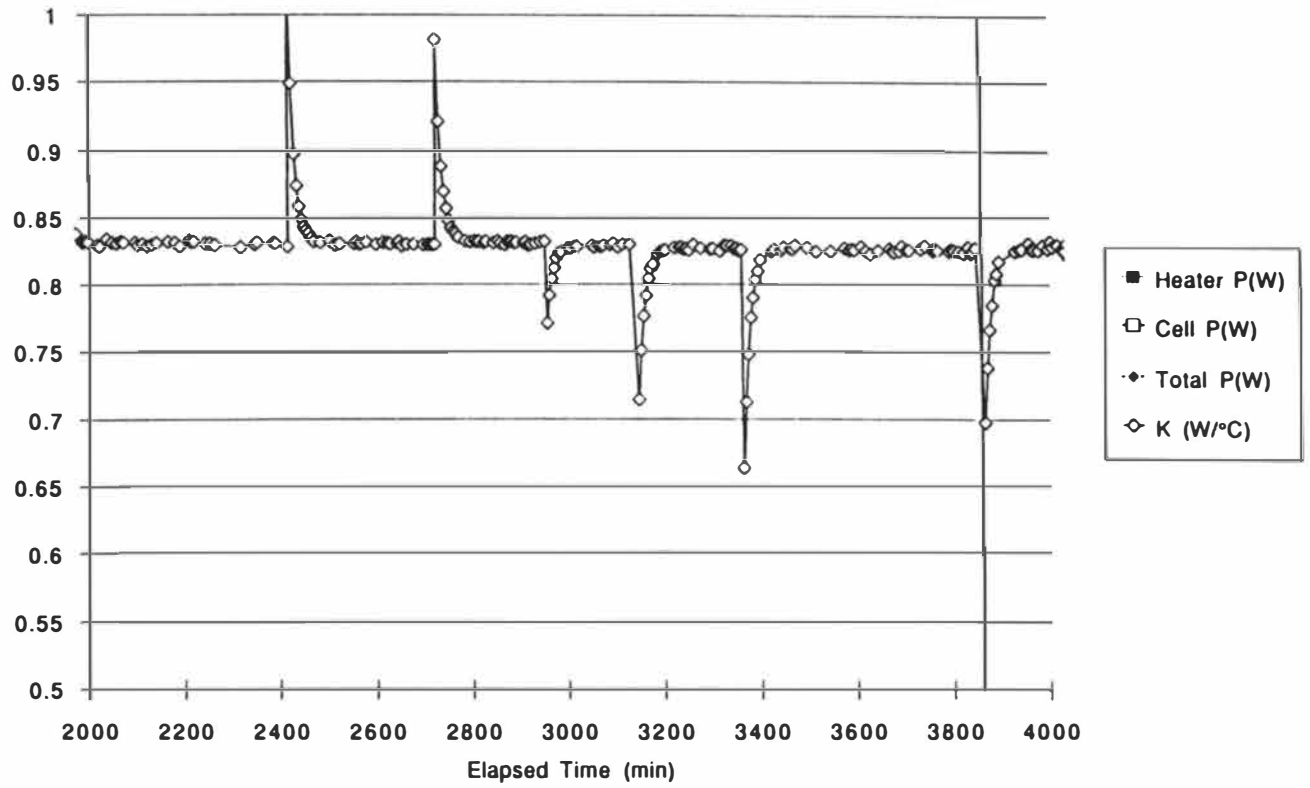
V.C. Linearity

The linear behavior of ΔT with the heat flux is illustrated in Fig. 8. All the data points lie on a straight line the slope of which is equal to the calibration constant. The plot clearly indicates that the calibration constant is independent of the input power level over a wide range of power values.

The variation of the calibration constant with the cell temperature is also of interest. It defines the linearity range of the calorimeter. The data shown in Fig. 9 indicate that it is practically independent of the cell temperature over a wide range of temperatures. It is interesting to note that the cell temperatures that are frequently used in this work fall into the range of ~ 50 to 60°C , which may have useful and practical implications.



(a)



(b)

Fig. 6. (a) The variation of joule heater, electrolysis, and total input power as a function of time during a calibration experiment by using an external thin sheet joule heater and (b) the corresponding values of the calibration constant K as a function of time and the input power level. It is clear that K is practically independent of the input power level as well as of time.

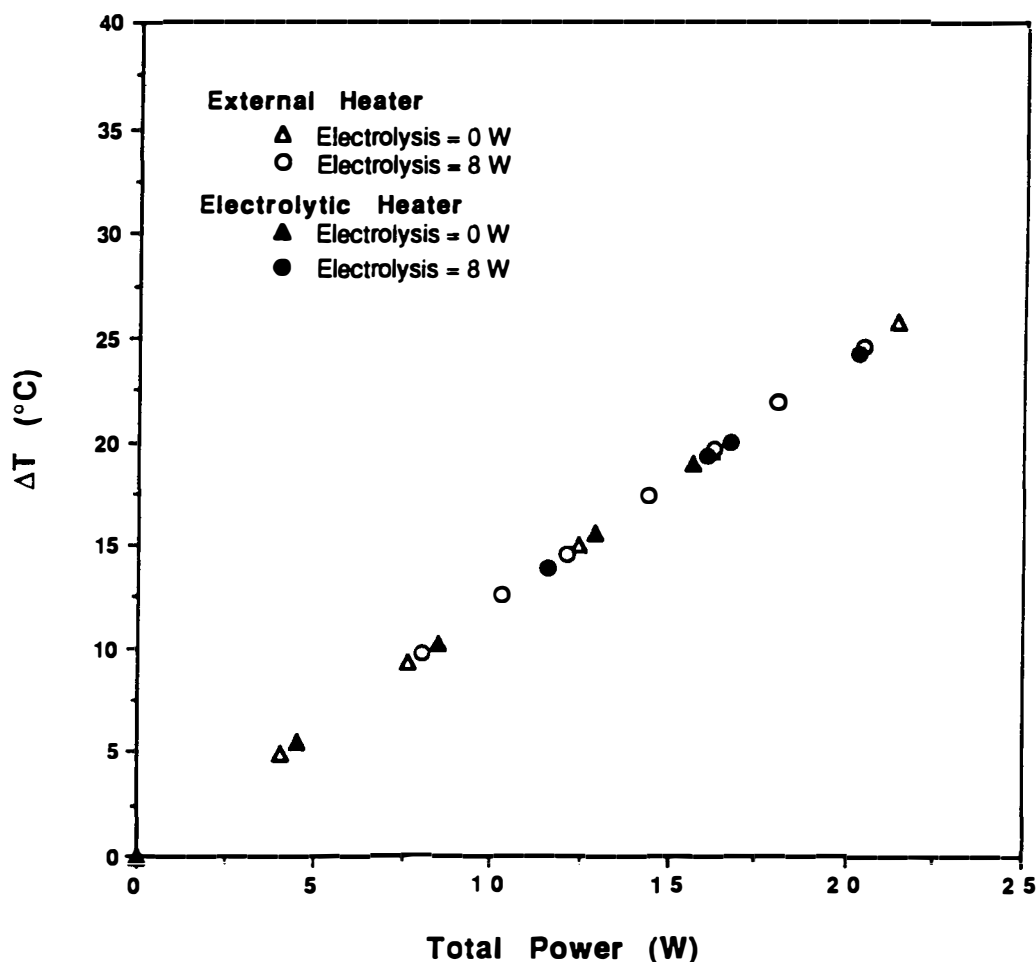


Fig. 7. Comparison between calibration results by using external thin sheet and internal electrolytic joule heaters both with and without the addition of electrolysis power. The data demonstrate that the calibration constant is practically independent of the method by which heat is introduced.

V.D. Sensitivity

The sensitivity values for the calorimeters usually vary between 1.1 and 1.2°C/W from calorimeter to calorimeter. Temperature differences between the inner and the outer aluminum cylinders are in the range of 10 to 30°C for electrolysis power maintained in the 10- to 25-W range. These high electrolysis power levels were chosen primarily for two reasons: (a) to drive the electrolysis to extreme conditions to achieve a very high activity for deuterium on the palladium cathode surface as well as to maintain a steep concentration gradient (i.e., high current density) for deuterium to diffuse rapidly into palladium and (b) to work in the range of parametric values where measurements of only large quantities are involved.

V.E. Dynamic Behavior and Time Constant

The dynamic behavior of the calorimeter during a cycle of abrupt power steps in the up and the down di-

rections is shown in Fig. 10. The response of the calorimeter is rather fast. The temperature difference ΔT almost immediately follows the change in the power level. After thermal equilibration is attained, the temperature remains flat, independent of time. The $1/e$ time constant for the calorimeter is ~ 13 min and does not seem to depend on the direction of the change in the power level. This is a reasonably short time to effectively follow and monitor changes in the thermal behavior of the deuterium-palladium system.

V.F. Reproducibility

Reproducibility is illustrated by comparing the dynamic behavior of two different calorimeters of identical design chosen at random among the eight calorimeters. The results are depicted in Fig. 11, which shows the normalized time-dependent temperature changes in two different calorimeters that have undergone power step changes from two different initial values, 14.5 and

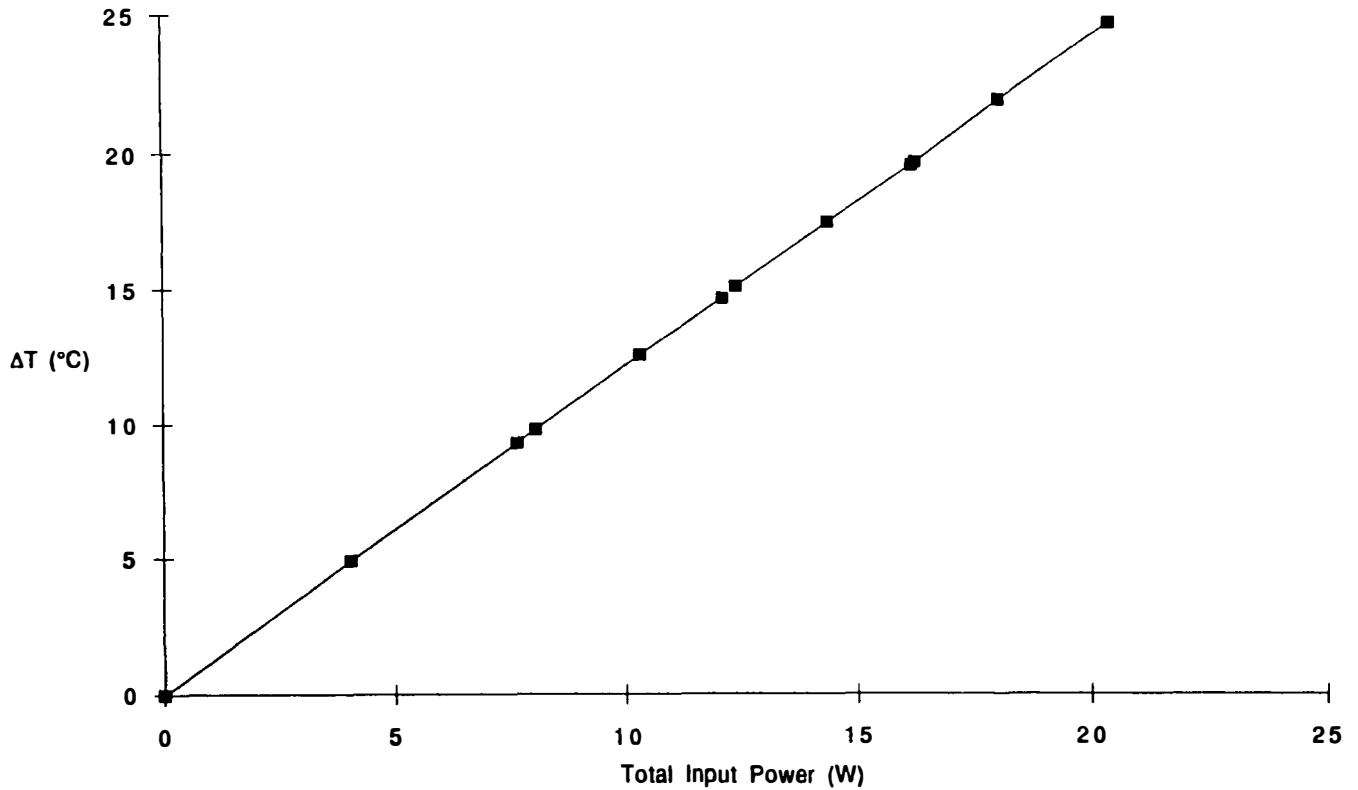


Fig. 8. Experimental data indicate that the calibration constant is linear with respect to the heat flux over a wide range of powers.

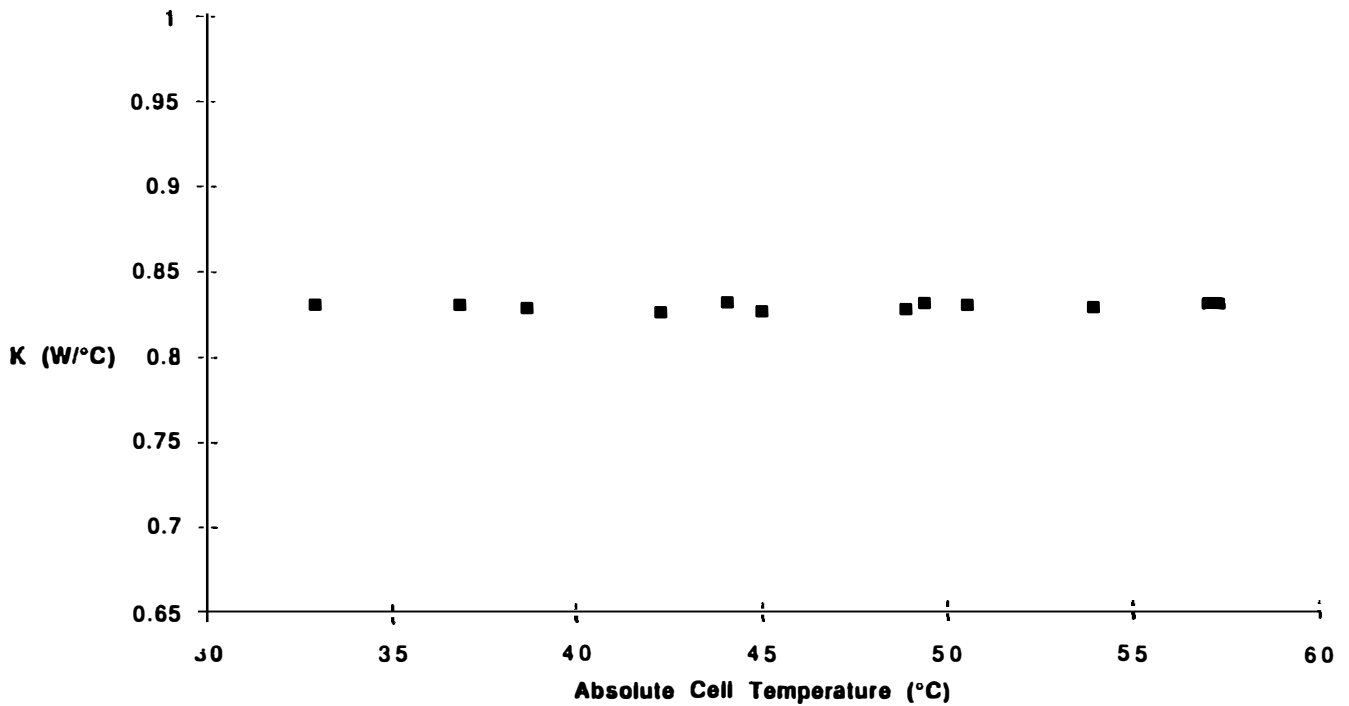


Fig. 9. Variation of the calibration constant with cell temperature. The data demonstrate that the calibration constant is independent of temperature over a very wide range.

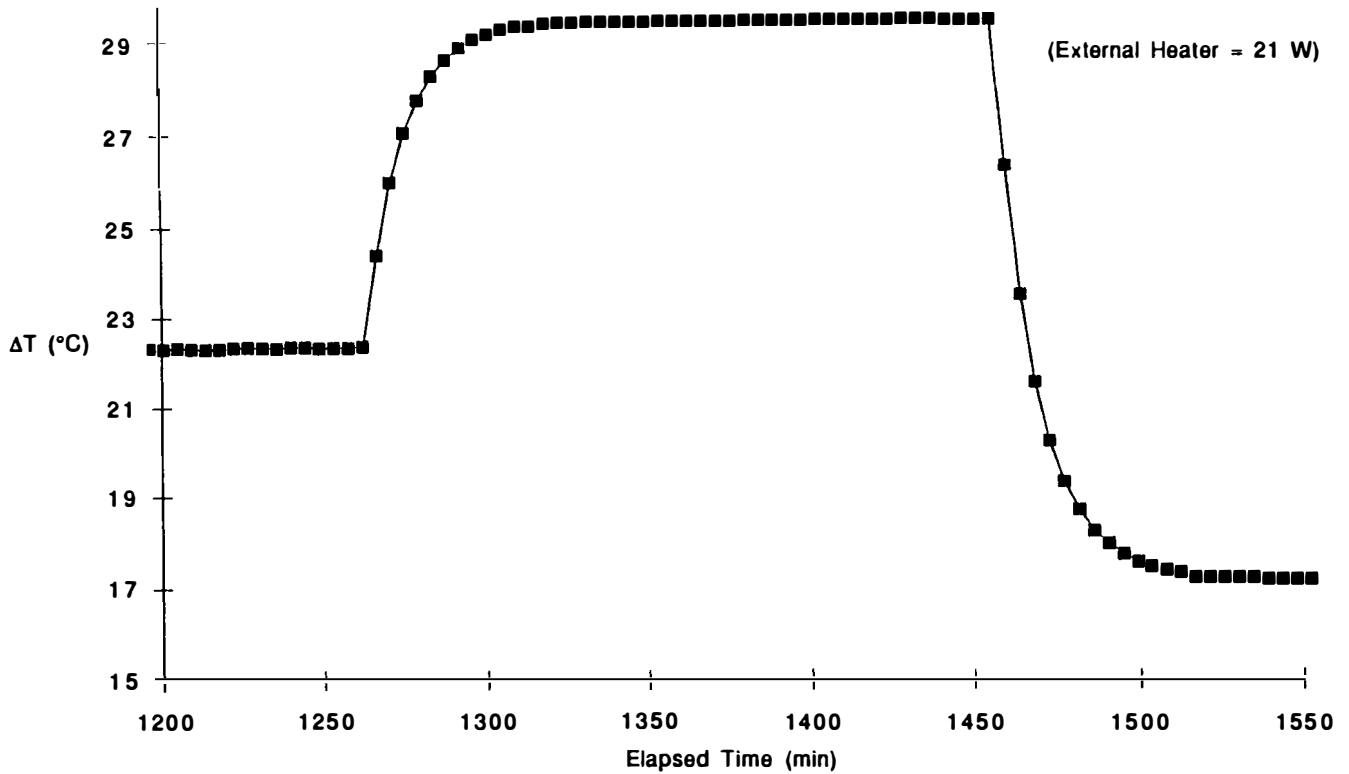


Fig. 10. The dynamic response of the calorimeter during a full cycle of increasing and decreasing power steps between different power levels.

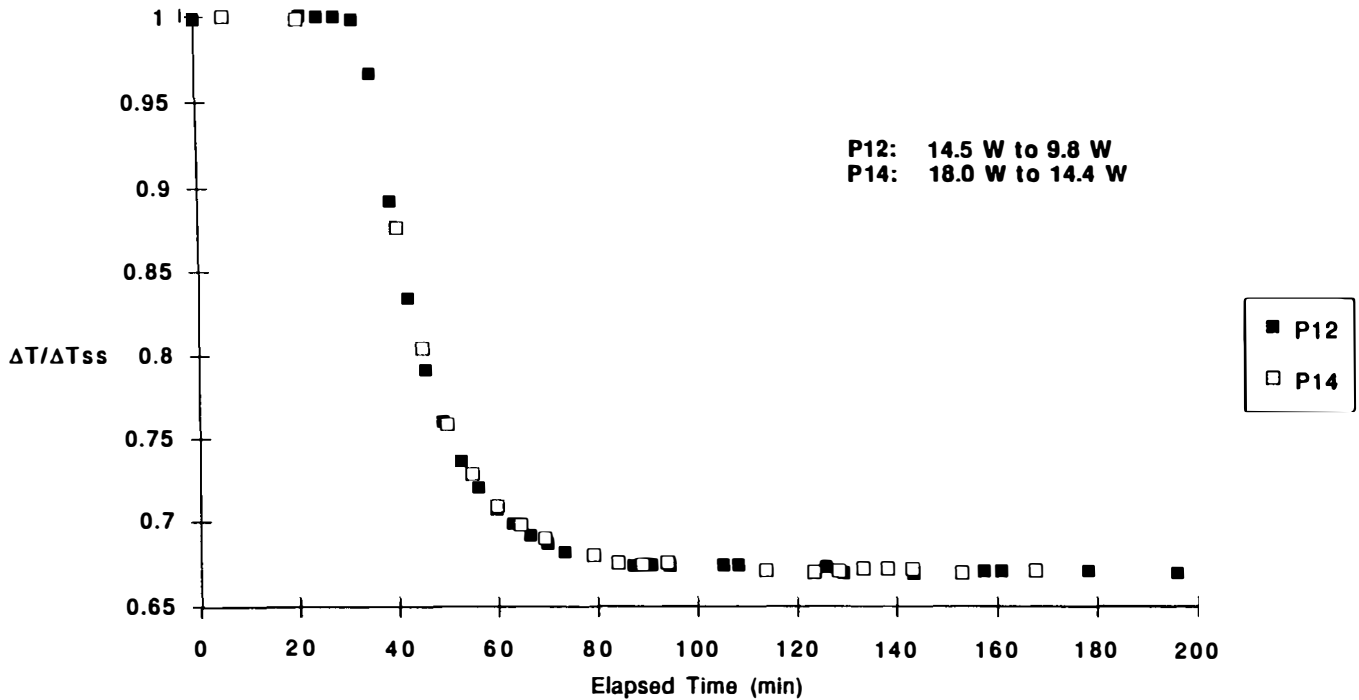


Fig. 11. The agreement on the reproducibility of the dynamic behavior of two different calorimeters undergoing power step changes from two different initial values to two different final values. The data represent the normalized temperature as a function of time and demonstrate the practically identical dynamic behavior of the calorimeters.

18.0 W, to two different final values, 9.8 and 14.4 W, respectively. Figure 11 clearly indicates that the dynamic behavior and the time constants of these two calorimeters were almost identical.

VI. DISCUSSION

The results presented here demonstrate that this isoperibolic design is suitable to study the thermal characteristics of electrochemical insertion of deuterium into palladium. The general design feature whereby heat is uniformly distributed throughout the inner aluminum cylinder makes it very attractive for this and other electrochemical studies as well as calorimetric measurements on chemical systems. It eliminates the need to do elaborate temperature profile studies to map out the thermal contours within the calorimeter.

The major components of the materials of construction for the calorimeter are aluminum metal and Al_2O_3 powder, both of which are capable of operating at much higher temperatures (possibly up to 600°C) than were employed in this study. This presents an opportunity to explore the high-temperature thermal characteristics of the deuterium-palladium or other deuterium-metal systems by using this calorimeter design. However, the construction materials used for the electrochemical cell will be the limiting factor that will determine the maximum temperature of operation.

The calorimeters have been calibrated by using three different modes of introducing calibration heat. The calibration constants were found to be independent of whether the calibration heat was supplied by an immersion joule heater, an electrolytic heater, or an external thin sheet joule heater. This provides flexibility to the calorimetry experiments by using this simple design, which is inherently fast to respond to step changes in the input power level.

The temperature distribution within the aluminum cylinders was also found to be uniform with respect to position. The bulky aluminum cylinders have been effective in diffusing the heat uniformly. This important advantage eliminates the ambiguities and the uncertainties in the measurements associated with the exact nature and the location of the heat source and the temperature probe. It also renders irrelevant the issue about the extent of stirring inside the electrochemical cell.

Sensitivity of this calorimeter design depends strongly on the spacing between the two aluminum cylinders and the thermal conductivity of the K-layer material. Thus, it is rather easy to adjust the sensitivity parameter by changing the spacing or the nature of the K-layer material. For a given thermal conductivity value of the K layer, the calorimeter sensitivity will increase as the spacing between the aluminum cylinders increases, and vice versa. Hence, the calorimeter design can be tuned according to the specific requirements of the chemical or the electrochemical system under study.

This argument is also valid for the calibration constant that is merely the reciprocal of the sensitivity. The calibration constants have been found to be independent of both time and the input power level over quite a wide range. This allows calorimetric experiments to be carried out over power levels of up to 22 W. The values of the calibration constants for the individual calorimeters ranged between 0.83 and $0.85 \text{ W}/^\circ\text{C}$ with uncertainties less than $\pm 0.5\%$. This level of precision is sufficient to study the thermal behavior of palladium during electrochemical insertion of deuterium where large values of power and temperature are monitored.

The calibration constant was also determined to be independent of the electrochemical cell temperature up to -60°C . This temperature is sufficiently high to have some practical implications.

VII. SUMMARY

An isoperibolic calorimeter was designed and fully characterized for electrochemical studies of deuterium insertion into palladium electrodes. The calibration constants obtained by several different methods agreed exceptionally well with each other and were found to be stable over a considerable range of power levels, cell temperatures, time, and the manner in which calibration heat was supplied.

This new design possesses many advantages that makes it very suitable to conduct careful studies of the thermal behavior of palladium cathodes during electrochemical insertion of deuterium. It can also be used for calorimetric studies in other electrochemical and chemical systems without the need for altering the basic design features. It is insensitive to the nature and the location of the heat source within the electrochemical cell. It has the capability of operating over a wide range of temperatures and power levels without loss of precision and linearity. In principle, this design can accommodate temperatures up to 600°C . The design also provides flexibility to allow changes in the spacing between the two aluminum cylinders to respond to specific system requirements such as calorimeter sensitivity.

ACKNOWLEDGMENTS

The authors were indebted to Roger Hart of Hart Scientific for valuable discussions and suggestions. This work was supported by the Electric Power Research Institute.

REFERENCES

1. W. HEMMINGER and G. HÖHNE, *Calorimetry: Fundamentals and Practice*, Verlag Chemie, Weinheim, Germany (1984).

2. S. SUNNER and M. MANSSON, "Combustion Calorimetry," *Experimental Chemical Thermodynamics*, Vol. 1, Pergamon Press, New York (1979).
3. E. CALVET, H. PRAT, and H. A. SKINNER, *Recent Progress in Microcalorimetry*, Pergamon Press, Oxford, England (1963).
4. J. M. SHERFEY and A. BRENNER, "Electrochemical Calorimetry," *J. Electrochem. Soc.*, **105**, 665 (1958).
5. N. A. GODSHALL and J. R. DRISCOLL, "Determination of Thermoneutral Potential of Li/SOCl₂ Cells," *J. Electrochem. Soc.*, **131**, 2221 (1984).
6. L. D. HANSEN and H. FRANK, "Kinetics and Thermodynamics of Chemical Reactions in Li/SOCl₂ Cells," *J. Electrochem. Soc.*, **134**, 1 (1987).
7. L. D. HANSEN, R. HART, D. M. CHEN, and H. F. GIBBARD, "High-Temperature Battery Calorimeter," *Rev. Sci. Instrum.*, **53**, 503 (1982).
8. M. FLEISCHMANN and S. PONS, "Electrochemically Induced Nuclear Fusion of Deuterium," *J. Electroanal. Chem.*, **261**, 301 (1989); see also M. FLEISCHMANN, S. PONS, and M. HAWKINS, Errata, *J. Electroanal. Chem.*, **263**, 187 (1989).
9. A. J. APPLEBY, Y. J. KIM, O. J. MURPHY, and S. SRINIVASAN, "Anomalous Calorimetric Results During Long-Term Evolution of Deuterium on Palladium from Alkaline Deuterioxide Electrolyte," *Proc. 1st Annual Conf. Cold Fusion*, Salt Lake City, Utah, March 28-31, 1990, p. 32, National Cold Fusion Institute (1990).
10. M. H. MILES, K. H. PARK, and D. E. STILWELL, "Electrochemical Calorimetric Evidence for Cold Fusion in the Palladium-Deuterium System," *J. Electroanal. Chem.*, **296**, 241 (1990).
11. C. D. SCOTT, J. E. MROCHEK, T. C. SCOTT, G. E. MICHEALS, E. NEWMAN, and M. PETEK, "Initiation of Excess Power and Possible Products of Nuclear Interactions During the Electrolysis of Heavy Water," *Proc. 1st Annual Conf. Cold Fusion*, Salt Lake City, Utah, March 28-31, 1990, p. 164, National Cold Fusion Institute (1990).
12. M. C. H. MCKUBRE, R. C. ROCHA-FILHO, S. I. SMEDLEY, F. L. TANZELLA, B. CHEXAL, T. PASELL, and J. SANTUCCI, "Calorimetry and Electrochemistry in the D-Pd System," *Proc. 1st Annual Conf. Cold Fusion*, Salt Lake City, Utah, March 28-31, 1990, p. 20, National Cold Fusion Institute (1990).
13. R. A. ORIANI, J. C. NELSON, S.-K. LEE, and J. H. BROADHURST, "Calorimetric Measurements of Excess Power Output During the Cathodic Charging of Deuterium into Palladium," *Fusion Technol.*, **18**, 652 (1990).
14. A. BELZNER, U. BISCHLER, S. CROUCH-BAKER, T. M. GÜR, G. LUCIER, M. SCHREIBER, and R. A. HUGGINS, "Two Fast Mixed-Conductor Systems: Deuterium and Hydrogen in Palladium: Thermal Measurements and Experimental Considerations," *J. Fusion Energy*, **9**, 219 (1990).
15. A. BELZNER, U. BISCHLER, S. CROUCH-BAKER, T. M. GÜR, G. LUCIER, M. SCHREIBER, and R. A. HUGGINS, "Recent Results on Mixed Conductors Containing Hydrogen and Deuterium," *Solid State Ionics*, **40/41**, 519 (1990).
16. N. S. LEWIS, C. A. BARNES, M. J. HEBEN, A. KUMAR, S. R. LUNT, G. E. McMANIS, G. M. MISKELLY, R. M. PENNER, M. J. SAILOR, P. G. SANTANGELO, G. A. SHREVE, B. J. TUFTS, M. G. YOUNGQUIST, R. W. KAVANAGH, S. E. KELLOGG, R. B. VOGELAAR, T. R. WANG, R. KONDRAT, and R. NEW, "Searches for Low-Temperature Nuclear Fusion of Deuterium in Palladium," *Nature*, **340**, 525 (1989).
17. G. M. MISKELLY, M. J. HEBEN, A. KUMAR, R. M. PENNER, M. J. SAILOR, and N. S. LEWIS, "Analysis of the Published Calorimetric Evidence for Electrochemical Fusion of Deuterium in Palladium," *Science*, **246**, 793 (1989).
18. D. E. WILLIAMS, D. J. S. FINDLAY, D. H. CRASTON, M. R. SENE, M. BAILEY, S. CROFT, B. W. HOOTON, C. P. JONES, A. R. J. KUCERNAK, J. A. MASON, and R. I. TAYLOR, "Upper Bounds on 'Cold Fusion' in Electrolytic Cells," *Nature*, **342**, 375 (1989).
19. G. KREYSA, G. MARX, and W. PLIETH, "A Critical Analysis of Electro-Chemical Nuclear Fusion Experiments," *J. Electroanal. Chem.*, **266**, 437 (1989).
20. M. SCHREIBER, T. M. GÜR, G. LUCIER, J. A. FERRANTE, J. CHAO, and R. A. HUGGINS, "Recent Measurements of Excess Energy Production in Electrochemical Cells Containing Heavy Water and Palladium," *Proc. 1st Annual Conf. Cold Fusion*, Salt Lake City, Utah, March 28-31, 1990, p. 44, National Cold Fusion Institute (1990).
21. S. PONS and M. FLEISCHMANN, "Calorimetry of Palladium-Deuterium System," *Proc. 1st Annual Conf. Cold Fusion*, Salt Lake City, Utah, March 28-31, 1990, p. 1, National Cold Fusion Institute (1990).
22. M. FLEISCHMANN, S. PONS, M. ANDERSON, L. J. LI, and M. HAWKINS, "Calorimetry of the Palladium-Heavy Water System," *J. Electroanal. Chem.*, **287**, 293 (1990).
23. B. Y. LIAW, P.-L. TAO, P. TURNER, and B. E. LIEBERT, "Elevated-Temperature Excess Heat Production in a Pd+D System," *J. Electroanal. Chem.*, **319**, 161 (1991).
24. M. FLEISCHMANN and S. PONS, "Calorimetry of the Pd-D₂O System: From Simplicity via Complications to Simplicity," *Phys. Lett. A*, **176**, 118 (1993).
25. E. STORMS, "Review of Experimental Observations About the Cold Fusion Effect," *Fusion Technol.*, **20**, 433 (1991).